ERDC/CRREL TR-18-16

US Army Corps
of Engineers®
Engineer Research and
Development Center

ERDC
ENGINEER RESEARCH & DEVELOPMENT CENTER

Engineering for Polar Operations, Logistics, and Research (EPOLAR)

Dynamic Modeling of Atmospheric Watch Observatory (AWO) Transport by Greenland Inland Traverse (GrIT)

Arnold J. Song and James H. Lever

September 2018

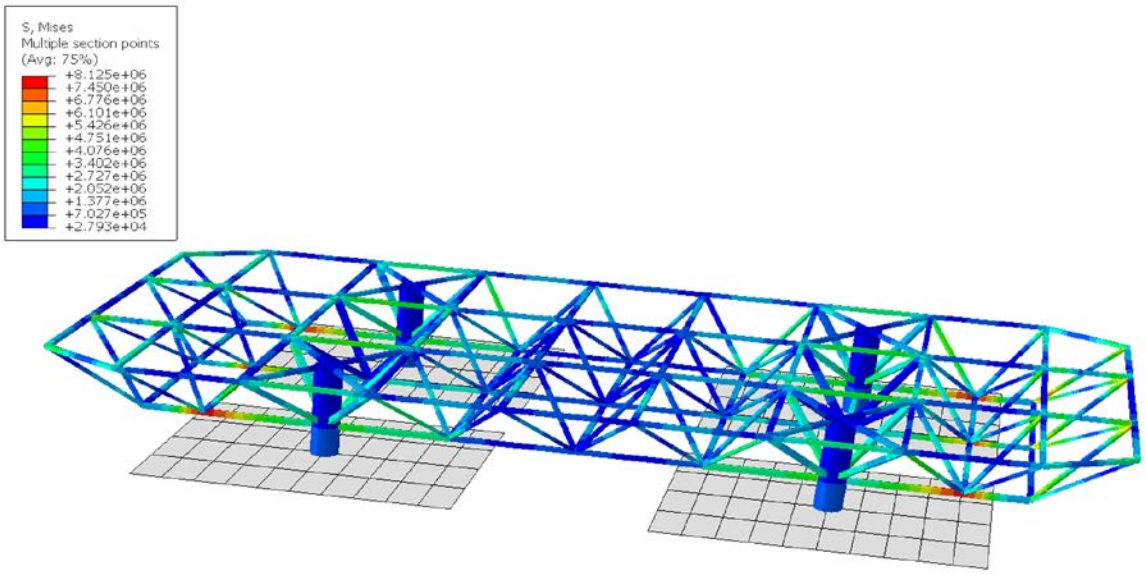

Cold Regions Research
and Engineering Laboratory

The U.S. Army Engineer Research and Development Center (ERDC) solves the nation's toughest engineering and environmental challenges. ERDC develops innovative solutions in civil and military engineering, geospatial sciences, water resources, and environmental sciences for the Army, the Department of Defense, civilian agencies, and our nation's public good. Find out more at www.erdc.usace.army.mil.

To search for other technical reports published by ERDC, visit the ERDC online library at http://acwc.sdp.sirsi.net/client/default.

Engineering for Polar Operations, Logistics,
and Research (EPOLAR)

ERDC/CRREL TR-18-16
September 2018

Dynamic Modeling of Atmospheric Watch Observatory (AWO) Transport by Greenland Inland Traverse (GrIT)

Arnold J. Song and James H. Lever

U.S. Army Engineer Research and Development Center (ERDC)
Cold Regions Research and Engineering Laboratory (CRREL)
72 Lyme Road
Hanover, NH 03755-1290

Final Report

Prepared for National Science Foundation, Office of Polar Programs (NSF-PLR),
Arctic Research Support and Logistics (RSL)
2415 Eisenhower Avenue
Arlington, VA 22230

Under Engineering for Polar Operations, Logistics, and Research (EPOLAR)
EP-ARC-14-12, “Support for GrIT”

Abstract

The National Science Foundation (NSF) plans to install a new Atmospheric Watch Observatory (AWO) to upgrade its research facilities at Summit Station, Greenland. The AWO welded-steel lower frame exceeds the size and weight limits for airlift transport; therefore, the only option to transport it to Summit is the Greenland Inland Traverse (GrIT) by using the newly developed Air Ride Cargo Sleds (ARCS). The study objectives were to determine whether GrIT can safely transport the AWO structure to Summit Station. The study addressed three assembly cases by estimating the transport-induced stresses and structural deformation by using the finite element method (FEM). The present analyses results strongly suggest that a preassembled AWO can safely travel to Summit via GrIT, which would allow NSF to realize cost and schedule savings.

Contents

Figures and Tables

Figures

Tables

Preface

This study was conducted for National Science Foundation, Division of Polar Programs (NSF-PLR), Arctic Research Support and Logistics (RSL), under Engineering for Polar Operations, Logistics, and Research (EPOLAR) EP-ARC-14-12, "Support for GrIT." The technical monitors were Ms. Renee Crain, RSL Associate Program Manager, and Mr. Patrick Haggerty, RSL Program Manager, NSF-PLR.

The work was performed by the Terrestrial and Cryospheric Sciences Branch (CEERD-RRG) and the Force Projection and Sustainment Branch (CEERD-RRH) of the Research and Engineering Division (CEERD-RR), U.S. Army Engineer Research and Development Center, Cold Regions Research and Engineering Laboratory (ERDC-CRREL). At the time of publication, Dr. John W. Weatherly was Chief, CEERD-RRG; Dr. Harley Cudney was Acting Chief, CEERD-RRH); Mr. J. D. Horne was Chief, CEERD-RR; and Mr. Jason Weale was the program manager for EPOLAR. The Deputy Director of ERDC-CRREL was Mr. David B. Ringelberg, and the Director was Dr. Joseph L. Corriveau.

COL Ivan P. Beckman was the Commander of ERDC, and Dr. David W. Pittman was the Director.

Acronyms and Abbreviations

2-D	Two-Dimensional
3-D	Three-Dimensional
AISC	American Institute of Steel Construction
ARCS	Air-Ride Cargo Sled(s)
AWO	Atmospheric Watch Observatory
CRREL	U.S. Army Cold Regions Research and Engineering Laboratory
EPOLAR	Engineering for Polar Operations, Logistics, and Research
ERDC	Engineer Research and Development Center
FEM	Finite Element Method
GrIT	Greenland Inland Traverse
HMW-PE	High Molecular Weight Polyethylene
HSS	Hollow Structural Sections
NOAA	National Oceanic and Atmospheric Administration
NSF	National Science Foundation
PLR	Division of Polar Programs
RSL	Arctic Research Support and Logistics
SPoT	South Pole Traverse

Unit Conversion Factors

Multiply	By	To Obtain
degrees (angle)	0.01745329	radians
feet	0.3048	meters
gallons (U.S. liquid)	3.785412 E-03	cubic meters
inches	0.0254	meters
miles (U.S. statute)	1,609.347	meters
miles per hour	0.44704	meters per second
pounds (force) per square foot	47.88026	pascals
pounds (force) per square inch	6.894757	kilopascals
pounds (mass)	0.45359237	kilograms
square feet	0.09290304	square meters

Executive Summary

The National Science Foundation (NSF) plans to install a new Atmospheric Watch Observatory (AWO) to upgrade its research facilities at Summit Station, Greenland. The AWO will consist of a building measuring 21 m (68 ft) long × 10 m (33 ft) wide × 6 m (21 ft) high that is supported by four telescoping legs. The AWO welded-steel lower frame exceeds the size and weight limits for airlift transport; therefore, the only option to transport it to Summit is the Greenland Inland Traverse (GrIT) by using the newly developed Air Ride Cargo Sleds (ARCS). NSF could also realize cost and schedule savings by preassembling the upper frame and exterior panels on the lower frame, provided that GrIT can safely transport the combined structure.

The study objectives were to assess whether GrIT can safely transport the AWO structure to Summit Station for three assembly cases: Case 1, the lower frame only; Case 2, the combined assembly composed of the upper and lower frames; and Case 3, a fully constructed building with exterior panels mounted to the full frame. The transport-induced stresses and structural deformation were calculated using the finite element method (FEM). The transport feasibility assessment used the calculated stresses and frame deformation for the transit over an isolated, 1 m (3 ft) high sastrugi, which is a particularly severe terrain case. Insofar as possible, the structural models were validated by comparing static (self-weight) analyses for Cases 1 and 2 with design-case stresses in the AWO lower frame.

The dynamic simulations revealed surprisingly strong coupling between pitch and roll motions of the AWO-ARCS system and the vibrational modes in the lower frame. Despite these dynamic effects, the present analyses strongly suggest that GrIT can safely transport the assembled AWO upper and lower frames with or without the exterior panels attached (Cases 2 and 3). GrIT transport of the lower frame (Case 1) could be safe, but strong dynamic coupling caused predicted stresses to be as high as design stresses with little margin for error. It seems likely that energy dissipation (damping) within the ARCS pontoons and into the snow would be much higher than modeled here. Also, when attached, the exterior panels are likely to increase damping for the AWO structure. These added damping sources will reduce dynamic coupling and thereby reduce maximum transport-induced stresses and displacements for all the transit cases considered.

Because preassembling the exterior panels could yield the largest cost savings but also entails the greatest risks, more detailed modeling is recommended once the panel attachment details are known. This additional modeling could also determine whether interior subsystems can be safely added before transport, contributing to further cost savings.

1 Introduction

1.1 Background

The National Science Foundation (NSF) operates Summit Station, at the height of the Greenland ice sheet, to conduct glaciology, atmospheric-physics, and climate-change research. In partnership with the National Oceanic and Atmospheric Administration (NOAA), NSF plans to install a new Atmospheric Watch Observatory (AWO) to upgrade its facilities at the Summit Station site. The AWO will consist of a building measuring 21 m (68 ft) long × 10 m (33 ft) wide × 6 m (21 ft) high that is supported by four hydraulically actuated, telescoping legs (Figure 1).

Figure 1. A three-dimensional (3-D) rendering of the planned AWO building installed at Summit Station (AECOM 2012). Four telescoping legs support the building through a lower, structural space frame. The building could be preassembled to include upper frame and exterior insulated panels prior to GrIT transport.

The AWO structure, which was designed by AECOM of Reston, VA, and Hugh Broughton Architects of London, is similar to modules designed for the British Antarctic Survey's Halley VI research station. Each telescoping leg can be lifted independently to allow periodic re-grading of the supporting snow foundation. This capability enables vertical repositioning of the building to stay on top of the snow surface as snowdrifts slowly accumulate at the site. If needed, the skis attached to the legs permit horizontal relocation of the entire building via towing by heavy equipment, but this relocation method is not meant for long distances over irregular terrain (Figure 2).

Figure 2. Halley VI modules being towed into place at the Halley Research Station of the British Antarctic Survey. These modules are structurally similar to the proposed AWO building and were designed to be towed on the skis attached to their telescoping legs.

The AWO's structure consists of a welded-steel lower frame onto which upper-frame (wall and roof) members are bolted (Figure 3). The lower frame consists of structural-steel tubing welded into a single, trusswork space-frame assembly, and it is designed to distribute the building's live load and dead weight onto the supporting legs (Figure 4). NSF plans to

have the lower frame fabricated in the United States or Europe and shipped by cargo vessel to Thule Air Base in northwest Greenland to stage it for transport to Summit. However, the dimensions of the completed lower frame exceed those of the cargo bay of an LC-130 aircraft used to fly cargo from Thule to Summit, which measures 2.7 m (8.8 ft) wide × 2.6 m (8.5 ft) high × 11.9 m (39 ft) long. Therefore, NSF plans to use the Greenland Inland Traverse (GrIT) to transport the AWO's completed lower frame to Summit. This over-snow transport option is feasible only if the stresses that would develop in the frame during transit over typical terrain are within allowable limits.

Figure 3. Combined assembly of the AWO lower and upper frames, including structural roof and telescoping legs (from AECOM 2012). Insulated panels bolt to these frame elements to create the exterior shell of the building.

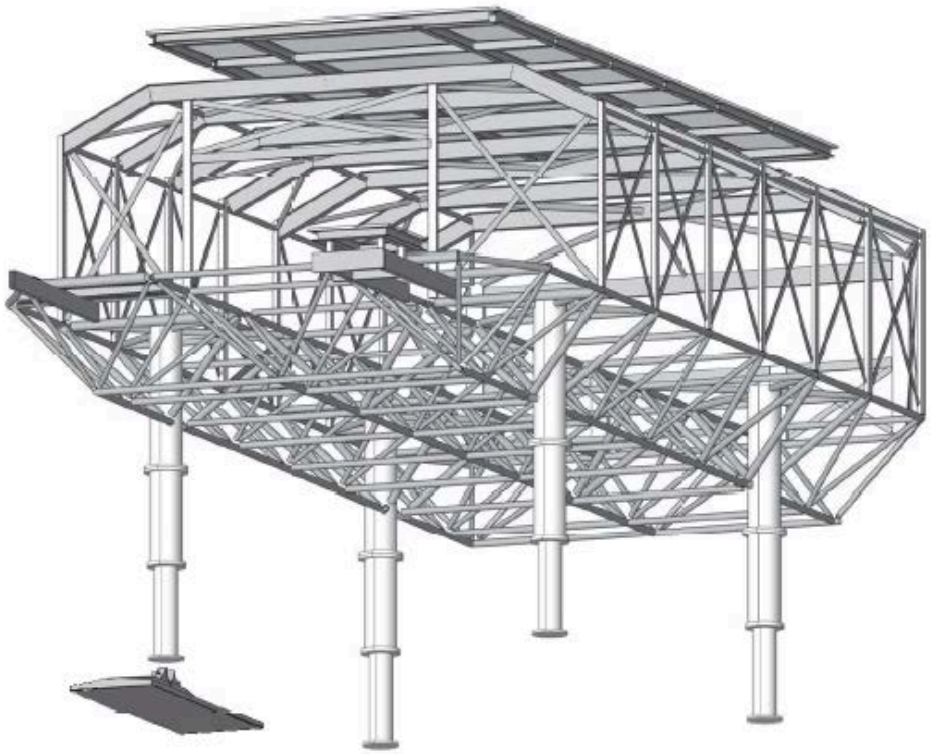

Figure 4. The AWO lower frame, a welded assembly of structural steel tubing (colors show the range of stresses from static self-weight of the frame as determined in the present analysis).

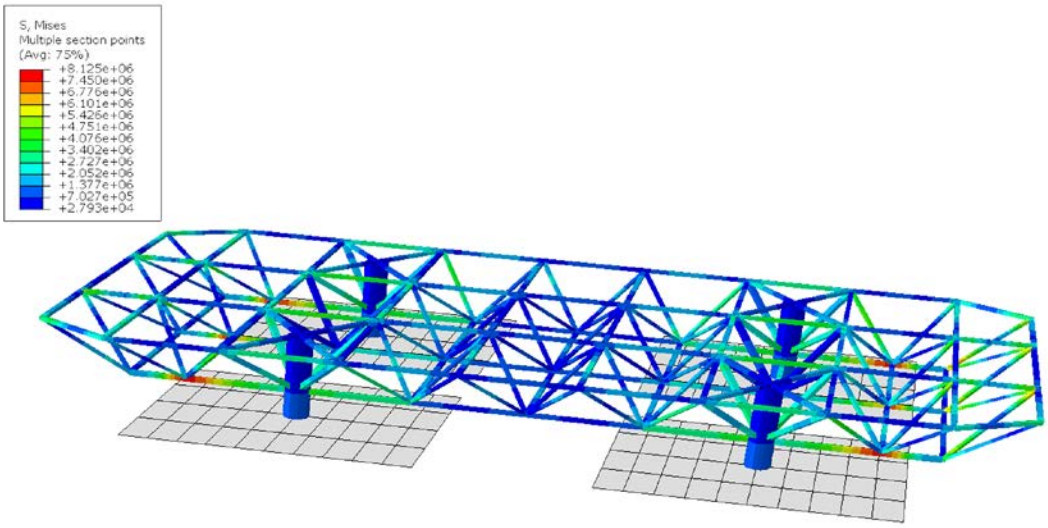

GrIT transports fuel and cargo over natural snow from just outside of Thule Air Base to Summit Station, a one-way distance of 1191 km (740 miles). Researchers at the U.S. Army Cold Regions Research and Engineering Laboratory (CRREL) have collaborated with GrIT and NSF's South Pole Traverse (SPoT) to develop lightweight fuel and cargo sleds to enhance the efficiency, and hence the economic payback, of heavy-haul traverses (Lever 2011; Lever and Weale 2012; Lever and Thur 2014; Lever et al. 2016a, 2016b). The Air Ride Cargo Sleds (ARCS) are an important product of this collaboration.

ARCS use air-filled pontoons to serve as a compliant, lightweight suspension between a wood-framed cargo deck and sheets of high molecular weight polyethylene (HMW-PE). Fabric pouches enclose the pontoons and structurally connect the deck to the HMW-PE sheets (Figure 5). Tractors tow assemblies of ARCS via spreader bars connected to steel tow plates at the front of each sheet. GrIT's ARCS have a 2,268 kg (5000 lb) tare weight and are designed to carry 11,340 kg (25,000 lb) of payload at 6.9 kPa (1.0 psi) ground pressure. The flat decks measure 5.0 m (15.7 ft) wide × 6.0 m (20 ft) long and can accommodate a range of payloads, including shipping containers, prefabricated modules, and loose-loaded cargo (Figure 6). The air-ride suspension cushions the payload over snow features, such as sastrugi; and low and uniform ground pressure helps to minimize towing resistance. Importantly, ARCS can be ganged together to transport payloads that are too large to airlift to Summit.

Figure 5. Rear 3-D view of ARCS designed to carry two 49,210 L (13,000 gal.) empty fuel tanks that weigh 10,886 kg (24,000 lb) each. Each wooden deck is 5.0 m (15.7 ft) wide × 6.0 m (20 ft) long and sits on six 0.6 m (2 ft) diameter × 6.0 m (20 ft) long single-chamber pontoons filled with air at 6.9 kPa (1 psi). The underlying sleds are 1.2 cm (½ in.) thick × 2.4 m (96 in.) wide HMW-PE sheets. The fabric pouches (*partially transparent blue*) each contain three pontoons (*red*) in separate compartments. Holes along the pouch sides allow them to be bolted to the deck and HMW-PE sheets, clamped with predrilled battens.

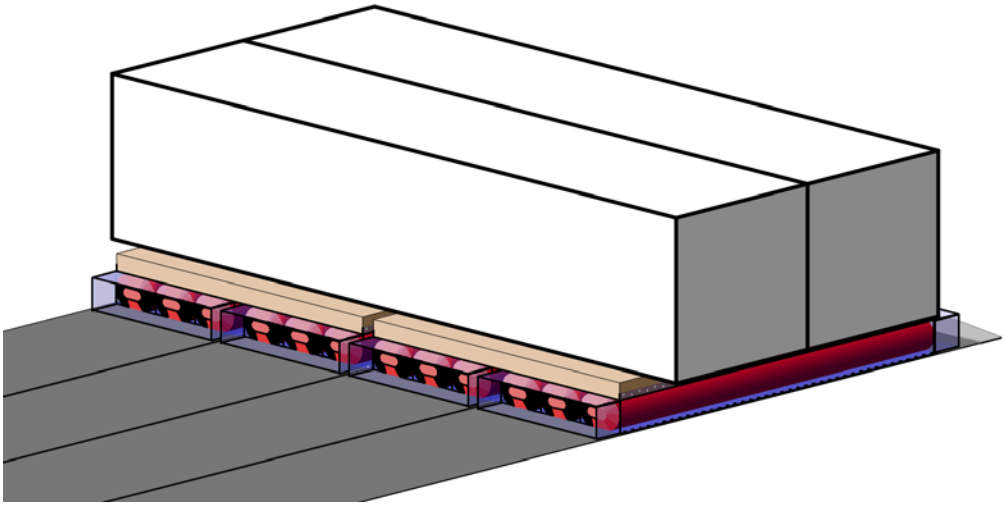

Figure 6. Four ARCS towed outbound on GrIT in 2012. The front pair of ARCS carried two 10,886 kg (24,000 lb) steel tanks. The rear pair carried a 6350 kg (14,000 lb) roller compactor and a tent enclosing tools and spare parts. GrIT12 successfully delivered the tanks and roller compactor to Summit Station on these ARCS.

1.2 Objectives

Field experience with ARCS on GrIT and SPoT has qualitatively demonstrated that they provide a very gentle ride for cargo contained on a single deck (Lever et al. 2016a). However, no measurements exist that quantify the motions or stresses imparted to payloads that span two or more ARCS. Because four ARCS would be needed for GrIT to transport the AWO's lower frame to Summit, NSF requested an estimate of the dynamic stresses likely to occur during transport to determine whether these would

be within allowable limits for the structure. If modeled transport-induced stresses exceeded allowable limits, this result would suggest that the lower frame be reinforced to enable GrIT transport.

In addition, costs and schedule savings would likely result if the entire AWO structure could be preassembled (in the United States, Europe, or at Thule Air Base) before being transported to Summit. Therefore, it was important to assess whether transport-induced stresses in the structure would be within tolerable limits for two additional cases: preassembly of the upper frame on the lower frame and preassembly of the exterior panels on the combined upper and lower frames.

The study objectives were thus to assess whether GrIT could safely transport the AWO structure for three assembly cases:

- Lower frame only (Case 1)
- Upper frame assembled on lower frame (Case 2)
- All exterior panels mounted to the assembled upper and lower frames (Case 3)

Based on the study results, NSF would then decide whether to reinforce or preassemble the AWO structure before transporting it to Summit on GrIT.

An important limitation of this study was the lack of participation by the designers of the AWO structure, AECOM. AECOM had expressed concern to NSF about GrIT transport in Case 3 possibly causing failure of the exterior-panel attachments. It was not possible to gain specific information about this concern or to determine design details or loading cases for the panels to compare with dynamic simulations. Also, while there was sufficient information to model the structure, the design loading cases for the lower frame could not be confirmed with the building designers to validate the model. These limitations shaped how the dynamic simulations were conducted and the results interpreted.

In particular, the lack of details on panel attachments and structural properties required special treatment. While preassembling the panels on the upper and lower frames could yield significant cost and schedule savings, potentially large transport-induced stresses could cause the attachments to fail and require expensive in-field repair. To overcome the lack of panel

details, the transport-induced displacements of the attachment points relative to each other were compared against the primary AWO design-case displacements, where the diagonally opposite legs were lifted as during jacking operations. The working assumption was that GrIT could safely transport the AWO structure with panels attached if the transport-induced displacements were no larger than the design-case displacements.

1.3 Approach

The motion and mechanical response of the AWO structure on ARCS traveling across rough sastrugi was simulated by using Abaqus, a commercial finite element method (FEM) solver package. These simulations yielded estimates for the time-varying stresses and displacements likely to occur during GrIT transport to Summit. The numerical AWO structural models were constructed using dimensions and weights provided by AECOM in its design submissions to NSF. The ARCS were modeled as spring-damper elements based on their air-filled pontoon construction. The individual sastrugi were represented as linear features of varying height and steepness, oriented at a preselected angle with respect to the travel direction of the AWO-ARCS sled assembly.

To validate the numerical model used in this analysis, the FEM-calculated stresses were compared against the design stresses reported by AECOM. As noted, the loading conditions of the AECOM structural analysis were not known, therefore one-to-one matching between this FEM model and the AECOM calculations was not possible.

2 Technical Approach and Methods

2.1 Structural model

This analysis used Abaqus to simulate the dynamic stress state of two configurations of an ARCS-mounted AWO structure as it traversed a snow bump (sastrugi): the lower frame only (Case 1) and a combined assembly of the lower and upper frames (Case 2). AECOM (2012) provided the structural-member types (cross-section specifications, beam dimensions, and steel type) and 3-D node locations needed to construct the models.

Based on joint details in AECOM (2012), all connections between members were assumed to be structurally rigid and sufficiently reinforced such that peak stresses would occur along the member rather than at the connections. This simplified modeling and was consistent with design loads in members reported in AECOM (2012). Each frame member was described in the numerical model with Abaqus beam elements that were discretized into five segments per member. The member cross-sectional geometries were defined according the standard structural sections specified in AECOM (2012). Appendix A provides details of the weights, dimensions, and components for the three cases modeled.

As noted, AECOM did not provide the details needed to model the AWO with the panels attached (Case 3). Therefore, the feasibility of transport in Case 3 was determined using the maximum strain values for each member and the resulting relative displacements at the panel connection points. In this way, the Case 2 model was used to assess Case 3 transport feasibility without actually needing to model the panel attachments.

2.2 ARCS model

Six single-chamber cylindrical pontoons, 6 m (20 ft) long with an unloaded diameter of 0.6 m (24 in.), support each ARCS deck (Figure 5). When compressed vertically, the pontoons act as nonlinear springs that provide restoring forces due to an increase in internal pressure caused by a decrease in bladder volume and an increase in contact area caused by the flattening of the tube cross section, as illustrated in Figure 7.

Figure 7. Cross section through a cylindrical pontoon of diameter *D*, showing change in shape as a result of uniform vertical compression, *z*, to produce restoring force *F*(*z*).

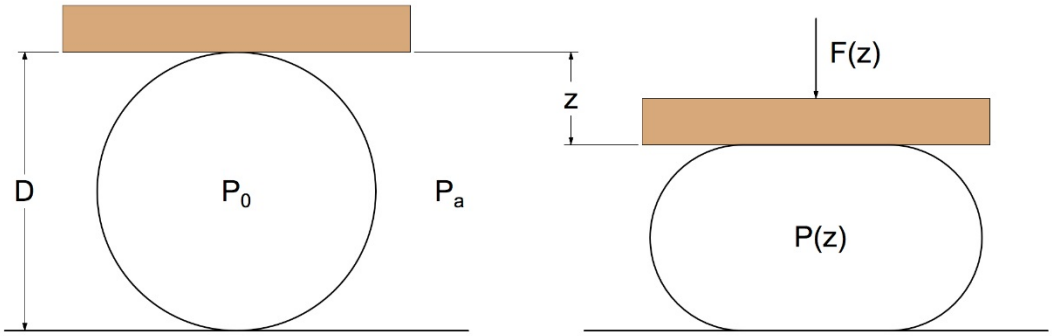

Because the pontoons consist of strong, polymer-coated woven fabric, a constant circumference during compression (i.e., the pontoon shell does not stretch) is assumed. Consequently, a simple closed-form solution exists to describe the restoring force, $F(z)$, for uniform compression:

$$F(z) = \left\{ \frac{P_0}{\left[1-\left(z/D\right)^2\right]^{\gamma}} - P_a \right\} \frac{\pi}{2} zL, \tag{1}$$

where

z = vertical displacement,
P_o = the absolute pressure inside the uncompressed pontoon,
P_a = atmospheric pressure,
L = pontoon length, and
γ = 1 for static (isothermal) compression or
γ = 1.4 for dynamic (adiabatic) compression.

The term inside the large brackets in Equation (1) represents the increased internal pressure resulting from compression z, and the multiplier $\frac{\pi}{2}z$ is the change in contact width.

To model non-uniform compression over rough snow, each pontoon is represented by 10 spring-damper elements (segments) governed by Equation (1) along with a procedure to determine the overall pontoon volume and hence internal pressure. The ARCS decks were modeled as rigid platforms, a good approximation given the soft compliance of the pontoons.

Field observations have shown that motions of heavily loaded ARCS decks dampen out quickly after passing over rough snow features. Lacking

measurements of these motions and physical descriptions of the damping processes, a simple linear damping was applied to each spring element proportional to the rate of change of *z*. The damping coefficient was tuned to produce a decay trace of about 1.5 cycles of vertical motion during initial settling of the model onto the snow surface. We acknowledge that the details of the damping behavior may not be an accurate representation in the model; however, the modeling behavior is adequate for evaluating the feasibility of ARC transport.

2.3 Terrain model

Long sections of the GrIT route consist of essentially flat snow. Nevertheless, fields of randomly distributed 3-D sastrugi (wind-sculpted snow features) exist along some segments, commonly with crest heights of 30–60 cm (1–2 ft) and wavelengths of 3–9 m (10–30 ft). Wind sculpting and packing of the snow surface cause the sastrugi to be strong enough to resist indentation by GrIT's ARCS (ground pressures of about 6.9 kPa [1.0 psi]). Thus, these sastrugi fields present a generally rough, non-deformable snow surface with respect to ARCS travel. However, the group of four ARCS transporting the AWO structure would extend over an area measuring about 10 m (33 ft) wide × 15 m (49 ft) long. This large footprint coupled with the compliant ARCS suspensions would largely accommodate the randomly rough snow surface. That is, for typical sastrugi fields encountered along GrIT's route, one would expect low transport-induced stresses on the AWO structure.

To assess transport-induced stresses for more extreme conditions, a test geometry was selected consisting of an isolated, two-dimensional (2-D) sastrugi with a 0.9 m (3.0 ft) crest height, a 1.8 m (5.9 ft) wavelength, and a sinusoidal profile with flat snow on either side and a rigid surface (no snow deformation). This provided approximately 1.5:1 as the steepest surface slope. The AWO-ARCS structural models were traversed at two approach angles to the sastrugi: 0° (normal to the sastrugi crest) and 45° (to generate simultaneous pitch and roll inputs to the sled assembly). The effects of sastrugi height were examined by including an analysis of a 30 cm (1.0 ft), 2-D sinusoidal sastrugi as a more gentle case.

Rather than create surface elements in Abaqus to represent the snow surface, the mathematical description of the surface profile was used as the lower node position for the spring elements that constituted the ARCS pontoons. This allowed much shorter computer run times than having to

solve for contact locations and forces between the spring and snow-surface elements at each time step. Variations in ARCS approach angles simply involved transforming the mathematical description of the snow surface to offset the crest.

2.4 Simulation characteristics

All simulations imposed a steady horizontal speed on the AWO-ARCS assembly of 2.2 m/s (5 mph), a common travel speed of the GrIT fleet. Linkages transferred the imposed speed to the center of the front two ARCS decks to allow the assembly to pitch and roll as it traversed the sastrugi in a manner similar to GrIT's ARCS. This kinematic constraint also eliminated the need to model ARCS sliding friction, which would affect only the force needed to tow the AWO-ARCS assembly, not its motion over the sastrugi.

Abaqus solved the motion of the AWO-ARCS assembly at real-time intervals of 0.1 sec by using an explicit forward Euler integration. Each member of the AWO structure was modeled by using a shear-flexible linear beam element with the degrees of freedom coming from axial, torsional, and bending deformation. These strains (and stresses) were interpolated linearly along the axial dimension of the beam. For the relatively straightforward simulations conducted here, the Abaqus results are expected to accurately reflect the simulated transport cases.

3 Model Results

3.1 Static validation

AECOM (2012), sheet numbers 60246845_S_101 and 60246845_S_102, provides tables of maximum axial forces in the lower-frame structural members under full live and dead loads for three design cases: C1, normal conditions (4 support legs); C2, loss of support in one leg (3 support legs); and C3, temporary jacking at designed jacking points (three supporting points). These are all static design cases, and design case C2 served as the benchmark for validating the Abaqus model.

Abaqus determines the sectional properties and weights from the user-specified cross-sectional geometry and materials; therefore, each of the numerical models included the self-weight of the elements. AECOM provided NSF with a spreadsheet listing weights of AWO materials and components. These weights were compiled into major assemblies that are consistent with the transport cases (Table 1). For the two transport case explicitly modeled in Abaqus, the weights agree quite well with those derived from AECOM's component weights. To estimate the design loading used by AECOM for its C2 design case, the calculated live load was based on 50 lb/ft^2 applied over the usable interior floor space of 2005 ft^2 (AECOM 2012). The static stresses were then calculated for the frame supported only by two diagonally opposite legs.

Table 1. Weights for AWO major assemblies and for the two transport cases modeled in Abaqus.

Assembly (Transport Case)	AECOM Assembly Weight, kg (lb)	Abaqus Model Weight, kg (lb)	Ratio of Abaqus Weight to Total Dead Weight plus Live Load
Lower frame (Case 1)	13,996 (30,856)	14,036 (30,943)	0.15
Upper and lower frames (Case 2)	23,838 (52,555)	24,927 (54,954)	0.27
Upper and lower frames plus exterior panels (Case 3)	47,851 (105,494)	Not modeled	0.51
Live load	45,473 (100,250)	Not modeled	0.49
Total dead weight plus live load (AECOM design case C2)	93,323 (205,744)	Not modeled	1.00

Table 2 compares the Abaqus-calculated stresses for the two modeled transport cases versus the AECOM design-case C2 stresses (AECOM 2012). In general, one would expect the static stresses in members to scale

with applied weight. For example, the Abaqus-calculated stresses for Case 1 should scale as the ratio of lower-frame weight to total design weight (namely 0.15, Table 1) if the weight difference was uniformly distributed on the members and offered no structural support.

As noted, it is not known how AECOM calculated design loads for AWO, for example, whether it distributed the live load uniformly or according to some occupancy plan. Also, AECOM only reported design loads for a quadrant of the lower frame, suggesting that they assumed two-plane symmetry for the lower frame structure, the dead-weight distribution, and the live-load distribution. Furthermore, by not reporting stresses in the upper frame elements, AECOM likely neglected the structural support provided by the upper frame and exterior panels when calculating design loads, a conservative assumption. Allowing for these uncertainties, the Abaqus-calculated stresses are compared here with those derived from AECOM's design case C2.

As shown in Table 2, AECOM reported design stresses for 61 members (probably assuming two-plane symmetry). In four of these members, Abaqus predicted stresses that differed by more than a factor of 10 from the weight-scaled ratio of 0.15. If these four members are excluded, the ratio of Abaqus-predicted stresses to design stresses averaged 0.13 ± 0.64, close to the expected value of 0.15 but with a large standard deviation.

Several quality-control checks were conducted for the Abaqus Case 1 model: element sectional properties, geometry of connecting nodes, element connectivity, frame weight, boundary conditions, etc. Through this process, it was discovered that the lower frame is not symmetric about either its fore–aft plane or side–side plane. This factor alone could account for the variations between the AECOM and Abaqus results. Another contributing factor could be that AECOM did not apply the live load uniformly across the frame. Nevertheless, these quality-control checks confirmed the accuracy of this structural model. The average Abaqus-modeled stresses (neglecting outliers) scale closely with the weight ratio, validating the numerical model. Note that even the highest Abaqus-predicted stresses are only about 10% of the specified steel yield stresses, and stresses in most elements are only 1%–2% of yield stress (290 MPa [42,061 psi]). These low stresses tend to magnify differences with design stresses. Note that the maximum AECOM-reported design stress, –181 MPa (26,252 psi) (Table 2), represents 62% of yield stress.

Table 2. AECOM C2 design stresses and Abaqus-calculated static stresses for diagonally opposite two-leg support of lower frame and combined upper and lower frames.

Member ID	AECOM Design Axial Stress (Pa)	Abaqus Static Stress, Case 1 (Pa)	Ratio of Case 1 Stress to Design Stress	Adjusted Ratio of Case 1 to Design Stress	Abaqus Static Stress, Case 2 (Pa)	Ratio of Case 2 Stress to Design Stress
B01	2.37E+06	−3.29E+07	−13.87		1.92E+06	0.81
B02	−1.75E+08	−3.65E+07	0.21	0.21	−2.25E+07	0.13
B03	−1.28E+08	−8.25E+06	0.06	0.06	−1.37E+07	0.11
B04	−3.13E+07	2.04E+07	−0.65	−0.65	−6.92E+06	0.22
B05	−9.00E+06	−1.30E+07	1.45	1.45	−2.57E+06	0.29
B06	−6.37E+07	−1.43E+07	0.22	0.22	−7.96E+06	0.12
B07	−7.56E+07	−7.03E+06	0.09	0.09	−7.32E+06	0.10
B08	−1.56E+07	1.73E+07	−1.11	−1.11	1.21E+07	−0.77
B09	−3.56E+07	−2.35E+06	0.07	0.07	−7.51E+06	0.21
B10	−3.30E+07	−3.82E+06	0.12	0.12	−9.75E+06	0.30
B11	−3.54E+07	−1.57E+07	0.44	0.44	−1.83E+07	0.52
B12	−2.10E+07	−6.72E+06	0.32	0.32	−1.31E+07	0.62
B13	−1.33E+07	1.79E+06	−0.13	−0.13	2.19E+06	−0.16
D01	1.78E+07	8.13E+06	0.46	0.46	1.64E+06	0.09
D02	−1.76E+08	−5.87E+06	0.03	0.03	−2.33E+07	0.13
D03	1.54E+08	9.29E+06	0.06	0.06	2.82E+07	0.18
D04	−1.37E+08	−5.43E+06	0.04	0.04	−1.70E+07	0.12
D05	−1.81E+08	−3.17E+06	0.02		−2.18E+07	0.12
D06	6.14E+07	−4.71E+06	−0.08	−0.08	8.61E+06	0.14
D07	−7.94E+07	−4.56E+06	0.06	0.06	−1.58E+07	0.20
D08	−1.49E+07	−1.08E+07	0.73	0.73	2.03E+07	−1.36
D09	4.26E+06	1.59E+07	3.73	3.73	4.20E+06	0.98
D10	−7.44E+07	−1.75E+07	0.24	0.24	−1.04E+07	0.14
D11	1.14E+08	2.04E+07	0.18	0.18	2.06E+07	0.18
D12	−1.17E+08	−1.13E+07	0.10	0.10	−1.73E+07	0.15
D13	−1.68E+08	−1.65E+07	0.10	0.10	−2.29E+07	0.14
D14	1.35E+08	8.69E+06	0.06	0.06	2.10E+07	0.16
D15	−1.09E+08	5.79E+06	−0.05	−0.05	−8.25E+06	0.08
D16	−3.63E+07	7.95E+06	−0.22	−0.22	−3.19E+06	0.09
D17	6.18E+07	−1.10E+07	−0.18	−0.18	5.81E+06	0.09
D18	−2.46E+07	1.10E+07	−0.45	−0.45	1.25E+06	−0.05
D19	6.63E+07	−1.01E+07	−0.15	−0.15	6.60E+06	0.10
D20	−1.34E+07	5.54E+06	−0.41	−0.41	3.56E+06	−0.26
D21	5.64E+07	4.46E+06	0.08	0.08	8.46E+06	0.15
D22	1.42E+07	1.63E+07	1.15	1.15	8.20E+06	0.58
D23	2.72E+07	−6.78E+06	−0.25	−0.25	6.34E+06	0.23

Table 2 (cont.). AECOM C2 design stresses and Abaqus-calculated static stresses for diagonally opposite two-leg support of lower frame and combined upper and lower frames.

Member ID	AECOM Design Axial Stress (Pa)	Abaqus Static Stress, Case 1 (Pa)	Ratio of Case 1 Stress to Design Stress	Adjusted Ratio of Case 1 to Design Stress	Abaqus Static Stress, Case 2 (Pa)	Ratio of Case 2 Stress to Design Stress
D24	3.08E+07	−7.70E+06	−0.25	−0.25	7.81E+06	0.25
T01	−9.23E+07	9.62E+06	−0.10	−0.10	−1.12E+07	0.12
T02	−4.36E+07	2.68E+07	−0.62	−0.62	−1.79E+07	0.41
T03	9.43E+07	1.67E+07	0.18	0.18	1.08E+07	0.11
T04	−2.89E+07	8.27E+06	−0.29	−0.29	−3.35E+06	0.12
T05	−2.15E+07	6.28E+06	−0.29	−0.29	−7.02E+06	0.33
T06	−3.81E+07	1.09E+07	−0.29	−0.29	−6.05E+06	0.16
T07	1.99E+07	1.52E+07	0.76	0.76	4.04E+06	0.20
T08	1.23E+08	1.45E+07	0.12	0.12	1.27E+07	0.10
T09	3.12E+07	6.84E+06	0.22	0.22	1.48E+06	0.05
T10	2.51E+06	1.10E+07	4.39		4.35E+06	1.73
T11	1.35E+08	2.42E+06	0.02		2.34E+07	0.17
T12	−2.94E+07	−1.74E+07	0.59	0.59	7.50E+06	−0.26
T13	9.03E+07	2.33E+07	0.26	0.26	2.28E+07	0.25
T14	6.37E+07	4.05E+06	0.06	0.06	2.14E+07	0.34
T15	−3.41E+07	−2.07E+06	0.06	0.06	3.79E+07	−1.11
T16	5.10E+07	−1.44E+06	−0.03	−0.03	1.20E+07	0.23
T17	−3.23E+07	4.63E+06	−0.14	−0.14	4.36E+06	−0.14
T18	−1.45E+07	5.91E+06	−0.41	−0.41	6.54E+06	−0.45
T19	9.34E+06	4.75E+06	0.51	0.51	6.67E+06	0.71
T20	2.24E+07	2.46E+06	0.11	0.11	3.07E+06	0.14
T21	4.06E+07	2.01E+07	0.49	0.49	6.36E+06	0.16
T22	5.42E+07	−2.34E+07	−0.43	−0.43	9.11E+06	0.17
T23	5.96E+07	1.75E+07	0.29	0.29	1.94E+07	0.32
T24	4.22E+07	1.47E+07	0.35	0.35	2.01E+07	0.48
Average			−0.03	0.13		0.16
Std. Dev.			1.98	0.64		0.42

Table 2 also compares Abaqus-predicted static stresses for Case 2 (upper and lower frame) with AECOM's C2 design stresses. For Case 2, the weight ratio is 0.27 (Table 1), yet the Abaqus-predicted stresses average 0.16 ± 0.42 without any significant outliers. Despite an 80% increase in self-weight, the average Abaqus-predicted stresses only increased by 20%. Apparently, the upper frame provides some structural support for the lower frame to carry the additional weight. It appears that AECOM may

have neglected the upper-frame structural benefit when determining the design loads in the lower frame.

Quality-control checks were also conducted for the Abaqus Case 2. These quality checks, performed in conjunction with the comparison of member axial stresses for both Cases 1 and 2, validate the Abaqus AWO model.

As noted, Case 3 (upper and lower frames with exterior panels attached) was not modeled explicitly. Nevertheless, the static Case 2 results identified the largest strains in the diagonal members across the sides of the upper frame (Figure 3), which correspond to the largest relative displacements of the panel-attachment locations and thus provide baseline values to assess transport feasibility of Case 3. The static Case 2 analysis showed a maximum strain of 6.6×10^{-5}, which corresponds to a displacement of 0.25 mm (0.01 in.) across the 3.8 m (150 in.) diagonal length. AECOM (2012) did not report design-case stresses or strains in the upper frame elements, but if one assumes that the strains would scale with weight, the maximum design-case diagonal strain and displacement would be 6.4 μm (2.5×10^{-4} in.) and 0.9 mm (0.037 in.), respectively. These strain and displacement values were used as the reference for assessing the transport-induced effects on the exterior panels.

3.2 Dynamic simulations

Dynamic simulations each began with the AWO-ARCS assembly undergoing damped vertical motion for 5 s to reach equilibrium ride height on the flat snow surface upstream of the sastrugi. The simulation then applied 2 s of horizontal acceleration to reach a steady speed of 2.2 m/s (5 mph), which it then maintained until the entire AWO-ARCS assembly passed over the sastrugi. The output from each simulation included, for each 0.1 s time step, axial stresses in each member, relative displacements of the nodes, and rigid-body motions of the structure. These data were interrogated for the maximum stresses and strains within the AWO structure, the locations of these stresses and strains, and the structure's position on the sastrugi when these maxima occurred.

The eight dynamic-simulation runs consisted of two sastrugi heights and two approach angles for each structural model, Case 1 and Case 2. Note that the 0° approach angle represents crossing the 2-D sastrugi perpendicular to the line of its crest. The case naming convention was as follows: Case (*number*).(*sastrugi height*).(*approach angle*). For example, Case

1.3.45 denotes Case 1 structural model (lower frame), 0.9 m (2.7 ft) high sastrugi approached at 45°. Table 3 summarizes the main results from the dynamic runs. Although the table includes the direction of maximum stress for each run, the magnitudes of the maximum tensile and compressive stresses were generally within about 10% of each other.

Figure 8 shows key results for Case 1.3.45, simulated AWO-ARCS transit of the lower frame over a 0.9 m (2.7 ft) sastrugi at a 45° approach angle. This run generated the highest element stresses. Note that the horizontal axes in Figure 8 are distance from the start of travel, which is equivalent to time based on the steady 2.2 m/s (5.0 mph) travel speed. The gray bands denote the locations where the front and rear ARCS were in contact with the sastrugi; these bands overlap owing to the 45° approach angle. While Case 1.3.45 developed the maximum stresses, the other lower-frame (Case 1) runs showed similar characteristics.

It is likely that this strong dynamic coupling is an artifact from an inaccurate damping model for the ARCS pontoons and their interaction with natural (deformable) snow. For these analyses, the linear damping in each ARCS spring element was adjusted to achieve about 1.5 cycles of damped heave (vertical) motion of the AWO-ARCS system during its initial settling on the snow surface.

Table 3. Summary of results from the eight dynamic-simulation runs of the ARO-ARCS system over a sastrugi, where max σ/σ_Y is maximum tensile (positive) or compressive (negative) stress anywhere in the structure during transit; max diagonal strain and displacement are diagonally across the openings in the sides of the upper frame; max pitch and roll are the rigid-body rotations of the structure fore–aft and side–side, respectively.

Run ID	AWO Structure	Sastrugi Height, m (ft)	Approach Angle, deg.	Max σ/σ_Y	Max Diagonal Strain	Max Diagonal Displacement, mm (in.)	Max Pitch, deg.	Max Roll, deg.
Case 1.1.0	lower frame	0.3 (1)	0	−0.23	N/A	N/A	0.22	0.02
Case 1.1.45	lower frame	0.3 (1)	45	0.13	N/A	N/A	0.10	0.10
Case 1.3.0	lower frame	0.9 (3)	0	−0.57	N/A	N/A	2.7	0.02
Case 1.3.45	lower frame	0.9 (3)	45	−0.61	N/A	N/A	0.70	0.74
Case 2.1.0	upper and lower frames	0.3 (1)	0	0.15	−7.8E−05	−0.305 (−0.012)	0.15	0.01
Case 2.1.45	upper and lower frames	0.3 (1)	45	0.12	−7.1E−05	−0.279 (−0.011)	0.07	0.06
Case 2.3.0	upper and lower frames	0.9 (3)	0	0.16	−7.8E−05	−0.305 (−0.012)	0.15	0.01
Case 2.3.45	upper and lower frames	0.9 (3)	45	−0.29	−2.3E−04	−0.889 (−0.035)	0.60	0.56

Figure 8. Case 1.3.45 results plotted against distance traveled from start: (*upper*) pitch and roll motions, (*middle*) maximum tensile and compressive stresses anywhere in the structure, and (*lower*) tensile and compressive stresses in the structural element that experienced the maximum stress. The *gray bands* denote the locations where the front and rear ARCS were in contact with the sastrugi.

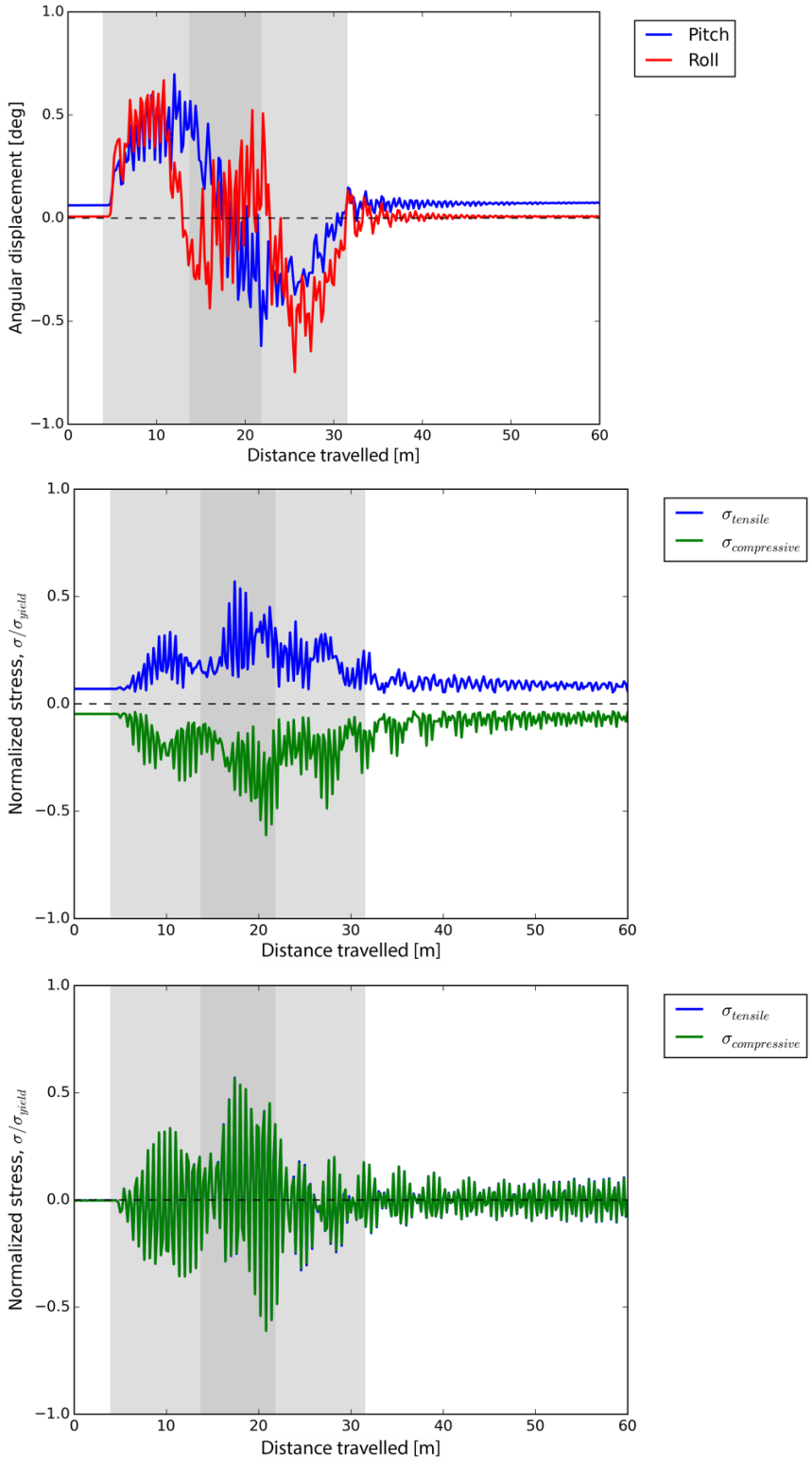

In reality, damping could be much stronger and is likely nonlinear with energy dissipation into the snow as an important contribution. Although the simulations predict maximum stresses that are well below yield stresses of the steel elements, they are sufficiently high (max $\sigma/\sigma_y \sim 0.6$) to raise concerns.

Without direct measurements of damping on ARCS, subsequent tuning of the damping coefficient simply to reduce this dynamic coupling would be arbitrary at best and is an issue left to address. The model results demonstrate that coupling between AWO-ARCS pitch and roll natural frequencies with AWO structural frequencies can feed energy from rigid-body motion of the assembly into the structure and increase stresses beyond the quasi-static values that result from the slow AWO-ARCS travel over sastrugi.

The middle and lower plots in Figure 8 show different stress signatures. The middle plot in Figure 8 is the time variation of the frame's global maximum stresses. The quasi-static signature resulting from slow motion over the sastrugi is fairly apparent in the plot. The offsets from zero represent maximum stresses anywhere in the structure on flat snow (self-weight stresses). By comparison, the bottom plot in Figure 8 shows the time-varying stress in the member that experiences the global maximum stress. This element is essentially unstressed on flat snow, and the aforementioned dynamic coupling dominates its stress signature.

Figure 9 shows the same simulation results for Case 2.3.45, where the AWO upper and lower frame assembly crosses the same sastrugi (0.9 m [3 ft] high, 45° approach angle). Immediately obvious in Figure 9 are the large reductions in high-frequency response compared with Figure 8. The addition of the upper frame on the lower frame increases mass and moment of inertia of the structure. While the nonlinear ARCS springs also increase in stiffness, the net result is to decrease significantly the roll frequency (from 3.0 Hz to 0.8 Hz) so that the roll signature in Figure 9 (upper) shows more clearly the two-cycle roll response over the sastrugi. The pitch frequency also reduces slightly (from 3.5 Hz to 3.1 Hz), but the large separation between pitch and roll frequencies apparently reduces the pitch response.

Figure 9. Case 2.3.45 results plotted against distance traveled from start: (*upper*) pitch and roll motions, (*middle*) maximum tensile and compressive stresses anywhere in the structure, and (*lower*) the time-varying tensile and compressive stresses in the structural element with the maximum global stress.

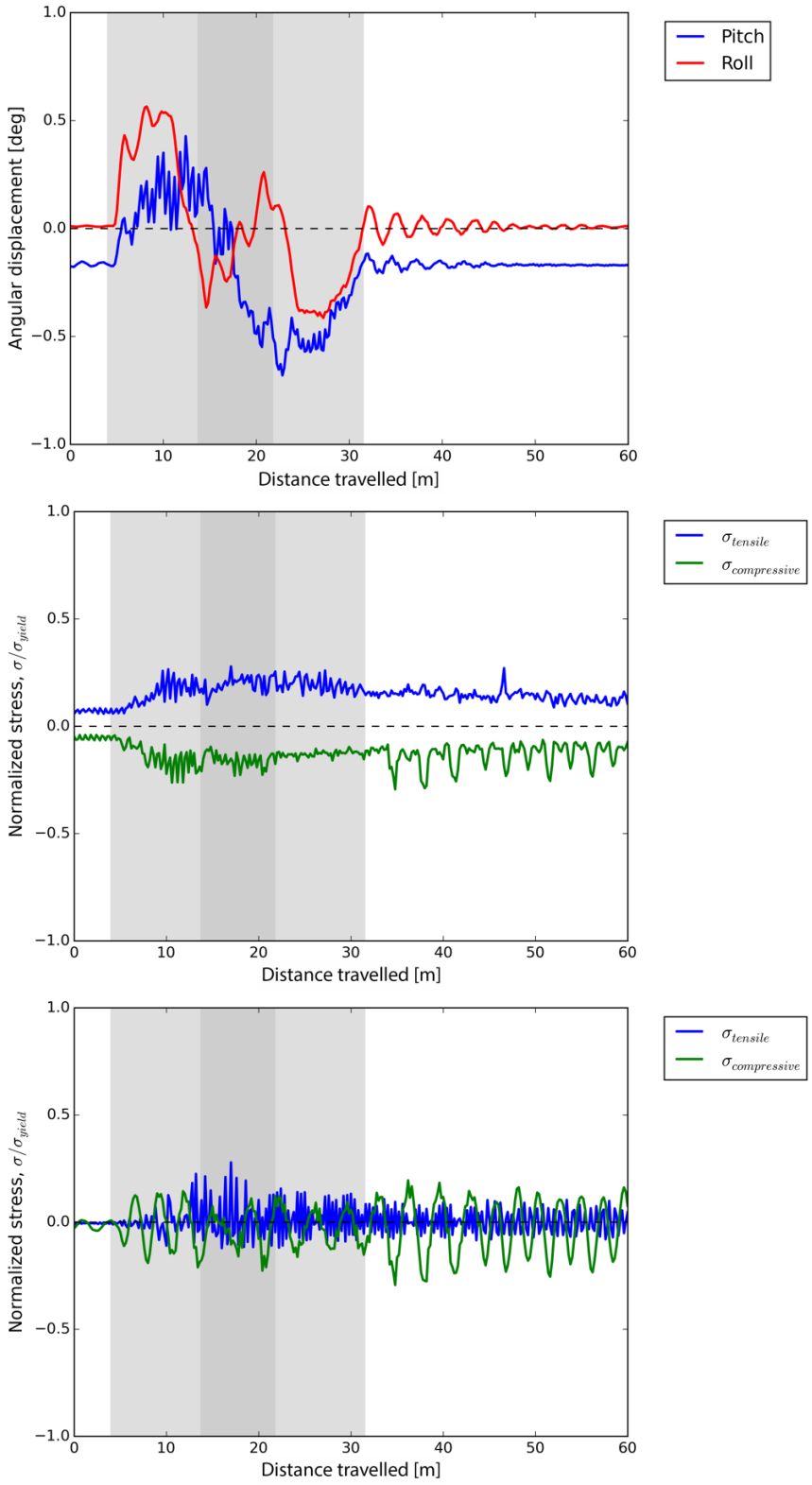

The dynamic stresses induced in the combined upper and lower frames contain significantly weaker high-frequency components and hence lower maximum stresses (Figure 9, middle and lower) compared with the dynamic behavior of the lower frame only as it traveled over the same sastrugi (Figure 8, middle and lower). The separation of rigid-body and structural natural frequencies appears to mitigate the energy transfer from the AWO-ARCS motion into individual structural members. Along with the damping from the air-filled pontoons and snow, the frequency separation can reduce the magnitude of the peak stresses experienced within the frame. Attaching exterior panels and internal subsystems onto the AWO frame may enhance this effect by further separating the natural frequencies.

Interestingly, the maximum stresses anywhere in the structure (Figure 9, middle) and in the most-stressed element (Figure 9, lower) show little signature of the slow response to motion over the sastrugi. High-frequency effects still dominate maximum stresses. For example, the stress signatures in the last 30 m (98 ft) of travel are dominated by ringing from the 0.8 Hz roll response. If energy dissipation on natural snow is higher than modeled here, actual transport-induced stresses could be significantly lower than those predicted. In the absence of dynamic coupling, transport-induced stresses would equal those generated by the quasi-static motion of the AWO-ARCS over the sastrugi, which produced maximum stresses of only 14% of yield stress (Figure 9, middle).

Despite the significant contribution of high-frequency effects, the predicted maximum stresses still remain below 27% of the yield stress (290 MPa [42,061 psi]). By comparison, maximum stress from the AECOM design case (two-legged support for the completed AWO building, Table 2) is 62% of yield stress. That is, predicted AWO-ARCS transport-induced stresses for the combined upper and lower frames are less than half of maximum design stresses, even including dynamic effects.

Recall that the upper-frame diagonal-element endpoint displacements are used as surrogate measures to assess the safety of GrIT transport of the AWO structure with the external panels installed. Predicted maximum strains and displacements across diagonals of the upper frame are quite small (Table 3). Case 2.3.45 produced the largest displacement, 0.89 mm (0.035 in.) compression across the 3.8 m (150 in.) diagonal element. While the AECOM design submissions did not include analysis of stresses and displacements of the upper frame, the Case 2 static analysis (Section

3.1) suggested that the AWO structure would experience 0.94 mm (0.037 in.) of diagonal displacement under its design case. Thus, the predicted transport-induced diagonal displacements are small and essentially the same as expected for the AECOM design case of two-leg support of the completed building.

4 Discussion and Conclusions

This study's objectives were to assess whether GrIT can safely transport the AWO structure to Summit Station for three assembly cases: lower frame only (Case 1); assembled upper and lower frames (Case 2); and exterior panels mounted to the assembled upper and lower frames (Case 3). The transport-induced stresses and displacements of AWO-ARCS transit over an isolated 0.9 m (3 ft) high sastrugi were modeled by using an Abaqus FEM solver to support the transport feasibility assessment. Insofar as possible, the structural models were validated by comparing the static (self-weight) analyses for Cases 1 and 2 with AECOM design-case stresses in the AWO lower frame.

The Case 1 results show a potential for strong dynamic coupling between rigid-body pitch and roll motions and structural response of the lower frame owing to the overlap of natural frequencies and low damping included in the Abaqus model. Although predicted maximum transport-induced stresses are similar to maximum design-case stresses ($\sigma/\sigma_y \sim 0.6$), they are sufficiently high to warrant further investigation for this AWO-ARCS transport option. Because dynamic effects dominate the Case 1 results, it seems likely that measurement and more realistic modeling of structural and ARCS damping will significantly reduce predicted maximum stresses. Because GrIT represents the only feasible transport option for the AWO lower frame, this additional investigation should precede a commitment to transport the lower frame without a supporting cradle.

The Case 2 results demonstrate that large reductions in dynamic effects result when rigid-body and structural frequencies are more broadly separated, in this case by increased mass and moment of inertia. With no change in damping, predicted maximum transport-induced stresses dropped in half to $\sigma/\sigma_y = 0.27$. The Case 2 simulations also revealed the slow, quasi-static response of the AWO-ARCS system to motion over the sastrugi. The very low stresses that result from that response ($\sigma/\sigma_y = 0.14$) attest to the benefits of ARCS transport of large assemblies, where several ARCS carry the structure and deform to accommodate sastrugi.

Because of the absence of exterior-panel attachment details, a combined upper and lower frame with panels assembly (Case 3) was not modeled in this effort. Rather, the maximum Case 2 transport-induced displacements of the opening over which the panels would attach was used as a proxy for

panel attachment integrity. These predicted displacements are small (maximum 0.89 mm [0.035 in.]) and are essentially the same as expected for the AECOM design case of two-leg support of the completed building. Therefore, even when dynamic effects are taken into account, one would expect the panel attachments to be no more severely stressed than when the completed AWO building is periodically jacked to accommodate snow-drifting at Summit.

The current results suggest that the panel attachments should survive transport on ARCS to Summit Station. Moreover, attaching the actual panels is likely to reduce displacements further because the total panel weight and moment of inertia will further separate natural frequencies of pitch and roll from structural frequencies, and the panels will probably dampen structural vibrations. Given the dominant role of high-frequency effects, the resulting transport-induced displacements of panel attachments could be substantially below the AECOM design case for the completed AWO structure.

Note that the Abaqus models did not include any damping of the structural-steel elements. Because dynamic effects produced the largest stresses, essentially any structural damping will reduce transport-induced stresses. Damping in steel-framed structures is difficult to estimate and generally warrants direct measurement. For AWO transport, energy losses from the structure into the ARCS will likely be important. Realistic modeling of structural damping should significantly reduce predicted dynamic response (i.e., stresses and displacements) for all transport cases compared with the current results.

The Abaqus FEM accurately simulated the simple transport cases considered for this assessment. More significant uncertainties relate to the simulation-case choices and the output measures used to assess safe transport. These uncertainties were mitigated by choosing a fairly extreme sastrugi height and comparing transport-induced stresses and displacements to design-case values.

AECOM's lack of participation and a lack of panel-attachment details limited the scope of the study. While the results suggest that the exterior panels could safely be added to AWO frames before transport, this conclusion cannot be directly confirmed by comparing stresses on the panels to allowable values. More detailed modeling should be conducted, preferably with

AECOM participation, once the attachment details are known. This additional modeling could also assess whether interior subsystems could be safely added before transport. However, the potential savings from more efficient construction prior to transport should first be estimated to justify additional modeling.

5 Recommendations

The present analyses strongly suggest that GrIT can safely transport the assembled AWO upper and lower frames with or without the exterior panels attached (Cases 2 and 3). GrIT transport of the lower frame (Case 1) could be safe, but strong dynamic coupling caused predicted stresses to be as high as design stresses with little margin for error. Recommendations for determining the best transport option for AWO on GrIT are as follows:

- Compile estimated cost and schedule savings from AWO preassembly for Cases 2 and 3 relative to Case 1 transport. These savings will help establish the level of additional modeling effort warranted to confirm safe GrIT transport for Cases 2 and 3.
- If potential cost savings justify additional analyses, conduct refined Abaqus simulations to confirm safe transport for the preferred structural configuration. Involve AECOM and selected AWO construction contractor, if possible.
- Measure and analyze the effects of energy dissipation of ARCS rigid-body motion (pontoon and snow energy losses). Higher rigid-body energy losses will significantly reduce transport-induced stresses by reducing energy transfer to structural vibrational modes, the dominant dynamic effect for all three transport cases. At a minimum, GrIT must transport the AWO lower frame to Summit (Case 1). Improved knowledge of energy dissipation is key to assuring that it can safely transport the lower frame without a reinforcing cradle.
- Because assembly of the exterior panels (and possibly some interior subsystems) on the combined upper and lower frames is likely to yield the greatest economic and schedule benefits but also to carry the greatest risks during transport, conduct additional analyses specifically to confirm safe transport for this configuration.

The results of this study show that safe transport of a fully assembled AWO using ARCS over typical Greenland terrain features is within the envelope of feasibility; but crucial details, such as the design load distribution and panel connections, are still missing from these structural analyses. Further study is necessary to ensure that transport stresses stay below safe levels for all conditions encountered while GrIT is en route.

References

AECOM. 2012. *AWO 100 Percent Drawings—Total Package*. Design package provided to NSF. Colorado Springs, CO: AECOM.

Lever, J. H. 2011. *Greenland Inland Traverse (GrIT): 2010 Mobility Performance and Implications*. ERDC/CRREL TR-11-16. Hanover, NH: U.S. Army Engineer Research and Development Center.

Lever, J. H., and P. Thur. 2014. *Economic Analysis of the South Pole Traverse*. ERDC/CRREL TR-14-7. Hanover, NH: U.S. Army Engineer Research and Development Center.

Lever, J. H., and J. C. Weale. 2012. High Efficiency Fuel Sleds for Polar Traverses. *Journal of Terramechanics* 49 (3–4): 207–213.

Lever, J. H., J. C. Weale, T. U. Kaempfer, and M. J. Preston. 2016a. *Advances in Antarctic Sled Technology*. ERDC/CRREL TR-16-4. Hanover, NH: U.S. Army Engineer Research and Development Center.

Lever, J. H., G. Phillips, and J. Burnside. 2016b. *Economic Analysis of the Greenland Inland Traverse*. ERDC/CRREL SR-16-2. Hanover, NH: U.S. Army Engineer Research and Development Center.

Appendix A: AWO Assembly Weights, Dimensions, and Component Details

Figure 4 illustrates the AWO lower frame assembly (Case 1) which is constructed as a welded assembly of hollow structural sections (HSS) steel tubing, namely HSS3.5x0.25, HSS4.5x0.237, HSS5.5x0.258, HSS12x4x3/8 and HSS6x3x1/2, arranged in space-frame configuration. The American Institute of Steel Construction (AISC) standardizes the dimensions and sectional properties of the HSS sizes. AECOM specified the steel grades to be ASTM A500 Grade B with 317 MPa (46,000 psi) and 290 MPa (42,000 psi) yield strengths for rectangular and round sections, respectively.

With the telescoping legs, the lower frame assembly weighs 14,061 (31,000 lb) and measures 21 m (68 ft) long × 10 m (33 ft) wide × 6 m (21 ft) high. As noted, the lower frame's weight and dimensions exceed the limits for LC-130 airlift to Summit: 9525 kg (21,100 lb) and 2.7 m (8.8 ft) wide × 2.6 m (8.5 ft) high × 11.9 m (39 ft) long.

Figure 6 shows the combined assembly of the AWO lower and upper frames (Case 2). The combined assembly weighs 24,948 kg (55,000 lb). The upper frame members consist primarily of similar steel tubing as the lower frame (HSS3.5x0.25, HSS4.5x0.237, HSS6x3x1/2, HSS12x4x3/8) plus structural beams W12x35 (ASTM A992, 345 MPa [50,000 psi] yield strength) and flat sections PL1/2x4 (no grade specified, 172 MPa [25,000 lb] yield strength assumed).

The Halley VI module shown in the lower image of Figure 2 approximates the appearance of the AWO structure preassembled for transport with the exterior panels attached to the combined lower and upper frames (Case 3). In this case, the assembly could weigh up to 47,854 kg (105,500 lb) depending on the internal subsystems added.

REPORT DOCUMENTATION PAGE

Form Approved
OMB No. 0704-0188

1. REPORT DATE *(DD-MM-YYYY)*	2. REPORT TYPE	3. DATES COVERED *(From - To)*
September 2018	Technical Report/Final	

4. TITLE AND SUBTITLE

Dynamic Modeling of Atmospheric Watch Observatory (AWO) Transport by Greenland Inland Traverse (GrIT)

5a. CONTRACT NUMBER

5b. GRANT NUMBER

5c. PROGRAM ELEMENT NUMBER

6. AUTHOR(S)

Arnold J. Song and James H. Lever

5d. PROJECT NUMBER

5e. TASK NUMBER
EP-ARC-14-12

5f. WORK UNIT NUMBER

7. PERFORMING ORGANIZATION NAME(S) AND ADDRESS(ES)

U.S. Army Engineer Research and Development Center (ERDC)
Cold Regions Research and Engineering Laboratory (CRREL)
72 Lyme Road
Hanover, NH 03755-1290

8. PERFORMING ORGANIZATION REPORT NUMBER

ERDC/CRREL TR-18-16

9. SPONSORING / MONITORING AGENCY NAME(S) AND ADDRESS(ES)

National Science Foundation, Office of Polar Programs
Arctic Research Support and Logistics (RSL)
2415 Eisenhower Avenue
Alexandria, VA 22314

10. SPONSOR/MONITOR'S ACRONYM(S)

NSF

11. SPONSOR/MONITOR'S REPORT NUMBER(S)

12. DISTRIBUTION / AVAILABILITY STATEMENT

Approved for public release; distribution is unlimited.

13. SUPPLEMENTARY NOTES

Engineering for Polar Operations, Logistics, and Research (EPOLAR)

14. ABSTRACT

The National Science Foundation (NSF) plans to install a new Atmospheric Watch Observatory (AWO) to upgrade its research facilities at Summit Station, Greenland. The AWO welded-steel lower frame exceeds the size and weight limits for airlift transport; therefore, the only option to transport it to Summit is the Greenland Inland Traverse (GrIT) by using the newly developed Air Ride Cargo Sleds (ARCS). The study objectives were to determine whether GrIT can safely transport the AWO structure to Summit Station. The study addressed three assembly cases by estimating the transport-induced stresses and structural deformation by using the finite element method (FEM). The present analyses results strongly suggest that a preassembled AWO can safely travel to Summit via GrIT, which would allow NSF to realize cost and schedule savings.

15. SUBJECT TERMS

Atmospheric Watch Observatory, Cushioned sleds, EPOLAR, Finite element method, Geographic information systems, Greenland, NSF; Polar traverse, Space frame, Strains and stresses, Terrain effects, Transportation--Cold weather conditions

16. SECURITY CLASSIFICATION OF:			17. LIMITATION OF ABSTRACT	18. NUMBER OF PAGES	19a. NAME OF RESPONSIBLE PERSON
a. REPORT	b. ABSTRACT	c. THIS PAGE			19b. TELEPHONE NUMBER *(include area code)*
U	U	U	SAR	41	